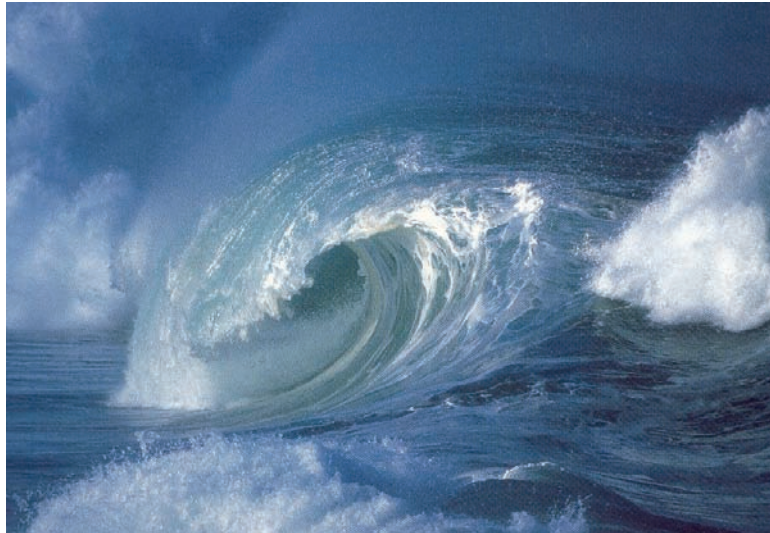


CROSS-SHORE TRANSFORMATION OF WAVE HEIGHT, ORBITAL MOTION, CROSS-SHORE AND ALONGSHORE CURRENT



B.T. Grasmeijer

version 1.3

University of Utrecht

MSc course Coastal and River Modeling

March 2006



Universiteit Utrecht

Abstract

This syllabus introduces a hydrodynamic model that can predict the cross-shore transformation of wave height, on- and offshore orbital motion, and time-averaged cross-shore and alongshore current. The set-up of the model in a spreadsheet is explained.

1. INTRODUCTION

Morphodynamic coastal profile models aim at predicting cross-shore bathymetric evolution by accounting explicitly for the various hydrodynamic processes involved (Roelvink and Brøker (1993)). With the increase in process knowledge and computing power, profile models have become standard tools in coastal management and are used for hind- and forecasting studies of nearshore bathymetry, often in response to human interference in the nearshore, for instance related to implementation of a shoreface nourishment. The models generally consist of three main modules. In the hydrodynamic module, the cross-shore evolution of wave height, orbital velocities and time-averaged (over many wave periods) cross-shore and alongshore currents is computed. These are then used as input in the sediment transport module. From the cross-shore gradients in the sediment transport rates, morphological changes are computed in the bed-update module, after which the whole procedure is repeated.

2. MODEL DESCRIPTION

2.1. WAVE TRANSFORMATION

The wave model consists of two coupled differential equation describing the time-averaged wave and roller energy balances. With the assumption of alongshore uniform bathymetry, the former reads

$$\frac{\partial}{\partial x} (E c_g \cos \theta) + D_{br} + D_{bf} = 0 \quad (1)$$

In a simple stepping forward scheme this can be represented by

$$E_{x+\Delta x} = E_x \frac{c_{g,x} \cos \theta_x}{c_{g,x+\Delta x} \cos \theta_{x+\Delta x}} - \frac{(D_{br} + D_{bf}) \Delta x}{c_{g,x+\Delta x} \cos \theta_{x+\Delta x}} \quad (2)$$

where x is the cross-shore direction, positive onshore, E is the wave energy, c_g the relative wave group velocity, θ is the angle of incidence, g is acceleration of gravity, ρ is the water density, D_{br} and D_{bf} are the wave energy dissipation by breaking and bottom friction, respectively. From Equation (2) the wave height can be determined using

$$E = \frac{1}{8} \rho g H^2 \quad (3)$$

Breaking-induced dissipation is given by Battjes and Janssen (1978):

$$D_{br} = \frac{1}{4} Q_b \rho g \frac{1}{T_p} H_m^2 \quad (4)$$

where T_p is the wave spectrum peak period, Q_b is the fraction of breaking waves following from an approximation of the original Battjes and Janssen (1978) formulation

$$Q_b = \exp \left(\frac{0.9698 \left(\frac{H}{H_m} \right)^2 - 1}{0.6574 \left(\frac{H}{H_m} \right)^2} \right) \quad (5)$$

where H_m is the maximum wave height following from

$$H_m = \frac{0.88}{k} \tanh \left(\frac{\gamma kh}{0.88} \right) \quad (6)$$

where k is the wave number $k = 2\pi/L$, h is the water depth, γ is the breaker criterion $\gamma = 0.76kh + 0.29$, based on calibrations. Dissipation by bed friction D_{bf} is of subordinate magnitude inside the surf zone where wave breaking dominates the dissipation.

$$D_{bf} = \frac{\rho f_w}{12\pi} \left(\frac{2\pi H}{T \sinh(kh)} \right)^3 \quad (7)$$

where f_w is the wave-related friction coefficient following from

$$f_w = \exp \left(-6 + 5.2 \left(\frac{A_b}{k_{s,w}} \right)^{-0.19} \right) \quad (8)$$

where A_b is the near-bed orbital excursion based on linear wave theory.

$$A_b = U_b \frac{T}{2\pi} \quad (9)$$

where U_b is the near-bed peak orbital velocity according to linear wave theory, see Equation (23), and T is the wave period.

At wave breaking, part of the organised wave energy is first converted into forward momentum flux to the roller. This region of aerated water appears as a wave makes the transition from nonbreaking to fully broken state. Svendsen (1984) was the first to account for this roller influence in the energy balance. According to Stive and De Vriend (1994), the energy balance for rollers is

$$\frac{\partial}{\partial x} (2E_r c \cos \theta) = -D_r + D_{br} \quad (10)$$

In a simple stepping forward scheme this can be represented by

$$E_{r,x+\Delta x} = E_{r,x} \frac{c_x \cos \theta_x}{c_{x+\Delta x} \cos \theta_{x+\Delta x}} + \frac{(-D_r + D_{br}) \Delta x}{2c_{x+\Delta x} \cos \theta_{x+\Delta x}} \quad (11)$$

where E_r is the roller energy density, D_{br} is energy dissipation by breaking as computed from Equation (1), D_r is the roller dissipation. Following Duncan (1981) and Deigaard (1993) the roller dissipation is modelled as:

$$D_r = \frac{2gE_r \sin \beta}{c} \quad (12)$$

The wave front slope β is usually assumed to be 0.1 or less (e.g. Reniers and Battjes (1997), Ruessink et al. (2001)). The time-averaged wave set-up and set-down follows from the time-averaged cross-shore momentum balance, including contributions due to waves, rollers and the cross-shore wind stress.

Equations (1) and (10) can be solved in the onshore direction on a simple forward stepping scheme for given bathymetry and offshore values of H_{rms} , T_p , θ and tide level. Linear wave theory is used to compute c and c_{gr} , and $\theta(x)$ is determined using Snell's law.

2.2. CROSS-SHORE FLOW

Probably the most important mechanism causing profile erosion during strong wave conditions is the offshore-directed steady current near the seabed, commonly referred to as undertow. Here, the time-averaged and depth-averaged undertow velocity \bar{u} is derived from the mass flux due to the wave motion (Q_w) and the mass flux due to the surface roller (Q_r).

$$\bar{u} = -\frac{Q_w + Q_r}{h_{trough}} \quad (13)$$

where $h_{trough} = h - H/2$

Using linear theory, Q_w is computed as

$$Q_w = \frac{E}{\rho c} = \frac{1}{8} \left(\frac{g}{c} \right) H^2 \cos \theta \quad (14)$$

The roller contribution Q_r is computed following Svendsen (1984)

$$Q_r = \frac{A}{T} = \frac{2E_r}{\rho c} \cos \theta \quad (15)$$

2.3. ALONGSHORE FLOW

The depth- and time-averaged alongshore current velocity \bar{v} is obtained from the 1-D depth-integrated and time-averaged alongshore momentum balance between wave, wind and tidal forcing, and bottom stress and lateral mixing

$$\frac{\partial S_{xy}}{\partial x} + \rho g h \frac{\partial h}{\partial y} - \tau_{s,y} = -\rho f_c \bar{v} |\bar{v}| + \rho \varepsilon \frac{\partial}{\partial x} \left(h \frac{\partial \bar{v}}{\partial x} \right) \quad (16)$$

where S_{xy} is the off-diagonal component of the radiation stress tensor (Longuet-Higgins and Stewart (1964)), h is the total water depth, $\tau_{s,y}$ is the alongshore wind stress, f_c is the current-related friction coefficient, \bar{v} is the time- and depth-averaged alongshore current velocity, x is the cross-shore coordinate, y is the alongshore coordinate, and ε is the depth-averaged eddy viscosity.

The wave forcing is the cross-shore gradient of S_{xy} . Using linear theory and assuming waves to be narrow banded in direction, S_{xy} is

$$S_{xy} = \frac{1}{8} \rho g H^2 c_{g,r} \cos \theta \sin \theta + 2E_r \cos \theta \sin \theta \quad (17)$$

where the terms on the right-hand side are the wave and roller contribution, respectively. Using (1) with $D_{bf} \ll D_{br}$, Equations (10) and (17) yield (Reniers and Battjes (1997), Ruessink et al. (2001))

$$\frac{\partial S_{xy}}{\partial x} = -\frac{D_r \sin \theta}{c} \quad (18)$$

Inclusion of the surface roller in Equation (18) causes a lag in the transfer of momentum to \bar{v} , thereby shifting the location of the maximum \bar{v} in the onshore direction compared to a no-roller model, consistent with laboratory (Reniers and Battjes (1997) and field observations (Ruessink et al. (2001)).

The alongshore-surface gradient $\partial h / \partial y$ is incorporated in Equation (16) to represent the alongshore water surface gradients related to two-dimensional flow systems (for example tide and wind-induced flow). The magnitude of the alongshore-surface gradient should be known a priori. The alongshore-surface gradient is estimated from tidal velocities at the offshore boundary (i.e. using Equation (16) by ignoring wave and wind forcing, and lateral mixing)

$$\frac{\partial h}{\partial y} = -\frac{f_c}{gh} \bar{v}^2 \quad (19)$$

The alongshore water surface gradient is assumed to be constant in the cross-shore direction.

The current-related friction coefficient f_c is given by

$$f_c = \frac{g}{C^2} \quad (20)$$

in which C is the Chezy coefficient,

$$C = \frac{18 \log(12h)}{k_a} \quad (21)$$

with k_a the apparent roughness as given by Van Rijn (1993).

Lateral mixing is included in Equation (16) as a diffusion term (Longuet-Higgins (1970)). Important sources for lateral mixing in the surfzone are breaking-induced turbulence (Battjes (1975)), depth variation in the cross-shore and alongshore velocities (Putrevu and Svendsen (1992)) and shear waves (Özkan-Haller and Kirby (1999)). However, the cross-shore distribution of ε is not well understood, and for simplicity, a cross-shore constant and time-independent ε is assumed.

2.4. ORBITAL VELOCITIES

Skewness of the near-bed cross-shore orbital velocity plays a central part in many cross-shore profile models. Waves in shallow water produce an onshore velocity associated with the wave crest that is stronger and of shorter duration than that due to a wave trough. This onshore velocity is more effective at moving coarser sediment than the offshore velocity. This effect is essential in predicting the shoreward transport of sediment during periods of beach recovery. It may be of equal importance as other cross-shore mechanisms such as the undertow (see e.g. Elfrink et al. (1999), Ruessink et al. (1998)).

A variety of wave theories have been devised to deal with the skewness of the wave orbital motion in deep or shallow water, all with their own range of application. In the present model Isobe and

Horikawa's (1982) parameterisation of a hybrid wave theory is used, which combines fifth-order Stokes wave theory and third-order cnoidal wave theory. The method by Isobe and Horikawa (1982) was originally formulated in terms of offshore wave conditions, but was later on modified by Grasmeyer and Van Rijn (1998) for local wave conditions. The method starts by computing the sum of the near-bed onshore and offshore peak velocity \hat{u} as

$$\hat{u} = 2 r U_b \quad (22)$$

where U_b is the peak near-bed orbital velocity computed using linear wave theory and r is a correction factor. The peak near-bed orbital velocity is computed as

$$U_b = \frac{\pi}{T} \frac{H}{\sinh(kh)} \quad (23)$$

In the present modified formulation the correction factor r is derived from the local wave conditions as follows:

$$r = -0.4 \frac{H}{h} + 1.0 \quad (24)$$

where H is the local wave height and h is the local water depth. Equation (24) was found by Grasmeyer and Ruessink (2003) using laboratory and field data with random waves.

The near-bed onshore peak orbital velocity u_{on} now follows from Isobe and Horikawa (1982)

$$\left(\frac{u_{on}}{\hat{u}} \right) = 0.5 + \left(\left(\frac{u_{on}}{\hat{u}} \right)_{\max} - 0.5 \right) \tanh \left(\frac{\left(\frac{u_{on}}{\hat{u}} \right)_a - 0.5}{\left(\frac{u_{on}}{\hat{u}} \right)_{\max} - 0.5} \right) \quad (25)$$

where the maximum skewness $\left(\frac{u_{on}}{\hat{u}} \right)_{\max}$ is given by

$$\left(\frac{u_{on}}{\hat{u}} \right)_{\max} = 0.62 + \frac{0.003}{\text{bed slope}} \quad (26)$$

and $\left(\frac{u_{on}}{\hat{u}} \right)_a$ by

$$\left(\frac{u_{on}}{\hat{u}} \right)_a = \lambda_1 + \lambda_2 \left(\frac{\hat{u}}{\sqrt{gh}} \right) + \lambda_3 \exp \left(-\lambda_4 \left(\frac{\hat{u}}{\sqrt{gh}} \right) \right) \quad (27)$$

with

$$\lambda_1 = 0.5 - \lambda_3 \quad (28)$$

$$\lambda_2 = \lambda_3 \lambda_4 + \lambda_5 \quad (29)$$

$$\lambda_3 = \frac{(0.5 - \lambda_5)}{\lambda_4 - 1 + \exp(-\lambda_4)} \quad (30)$$

$$\lambda_4 = \begin{cases} -15 + 1.35 \left(T \sqrt{\frac{g}{h}} \right), & T \sqrt{\frac{g}{h}} \leq 15 \\ -2.7 + 0.53 \left(T \sqrt{\frac{g}{h}} \right), & T \sqrt{\frac{g}{h}} > 15 \end{cases} \quad (31)$$

$$\lambda_5 = \begin{cases} 0.0032 \left(T \sqrt{\frac{g}{h}} \right)^2 + 0.000080 \left(T \sqrt{\frac{g}{h}} \right)^3, & T \sqrt{\frac{g}{h}} \leq 20 \\ 0.0056 \left(T \sqrt{\frac{g}{h}} \right)^2 - 0.000040 \left(T \sqrt{\frac{g}{h}} \right)^3, & T \sqrt{\frac{g}{h}} > 20 \end{cases} \quad (32)$$

It is noted that Equation (32) contains a typing error in the paper of Isobe and Horikawa (1982). This equation is continuous for $T(gh)^{1/2} = 20$ and not 30 (see Equation 19 in Isobe and Horikawa (1982)).

The laboratory and field data used in this study showed that the influence of bed slope on the maximum skewness is negligible. Instead, Grasmeyer and Ruessink (2003) suggest that the maximum skewness is related to h/L as

$$\left(\frac{u_{on}}{\hat{u}} \right)_{\max} = -2.5 \frac{h}{L} + 0.85 \quad (33)$$

with

$$0.62 \leq \left(\frac{u_{on}}{\hat{u}} \right)_{\max} \leq 0.75 \quad (34)$$

It should be kept in mind that Equation (33) merely serves as an upper limit to the skewness; in our experience, this upper limit is hardly ever reached.

The offshore peak orbital velocity, u_{off} , equals $u_{off} = \hat{u} - u_{on}$.

The present model includes a sinusoidal distribution of the instantaneous velocities during the forward and backward phase of the wave cycle. The duration period of each phase is corrected to obtain zero net flow over the full cycle. This is different from the original approach of Isobe and Horikawa (1982) who accounted also for a vertical skewness.

3. SPREADSHEET MODEL

It is relatively easy to build the wave height and cross-shore current module of the above-described hydrodynamic model into an Excel spreadsheet.

3.1. SET-UP OF THE SPREADSHEET MODEL

Create columns with the parameters given in Table 2. An example of how the spreadsheet looks like is shown in Figure 1. It is convenient to place the free model parameters k_{sw} (wave-related roughness height) and β (steepness of wave front) in separate cells. Place the constant water density ρ also in a separate cell. The free model parameters and constant are referred to using an absolute column and absolute row (Table 1). Absolute cell reference means the exact address of a cell, regardless of the position of the cell that contains the formula. An absolute cell reference takes the form $\$A\1 .

Table 1. Absolute and relative cell references

$\$A\1 (absolute column and absolute row).
$A\$1$ (relative column and absolute row)
$\$A1$ (absolute column and relative row)
$A1$ (relative column and relative row)

3.2. WAVELENGTH

The wavelength L is based on linear wave theory and is necessary to compute the wave number $k = 2\pi / L$. The three L columns are necessary to iterate to the correct wavelength. The first L column contains the following equation based on linear wave theory

$$L = \frac{gT^2}{2\pi} \tanh(kh) \quad (35)$$

The second L column contains an initial value for the wavelength and the column L_{error} contains the squared difference between the first and second L columns. The cell below the L_{error} column contains the sum of squared differences. Iteration is done by minimizing the sum of squared differences by changing the cells in the second L column (Figure 2).

3.3. PEAK NEAR-BED ORBITAL MOTION

The peak near-bed orbital velocity and orbital excursion are based on linear wave theory and is necessary to compute the dissipation by bed friction.

$$U_b = \frac{\pi}{T} \frac{H}{\sinh(kh)} \quad (36)$$

$$A_b = u_{linear} \frac{T}{2\pi} \quad (37)$$

3.4. WAVE GROUP AND WAVE PHASE CELERITY

The wave phase celerity c and wave group celerity c_g are computed as follows

$$c = \frac{L}{T} \quad (38)$$

$$c_g = nc \quad (39)$$

where n is the ratio of wave group and wave phase celerity following

$$n = 0.5 \left(1 + \frac{2kh}{\sinh(2kh)} \right) \quad (40)$$

Table 2. Parameters necessary in spreadsheet model to compute cross-shore transformation of wave heights and cross-shore current velocities

Parameter	Description
x	horizontal distance in x-direction
dx	step in x direction
z	bed level
h	water depth
H	wave height
T	wave period
L	wave length
L	wave length (for iteration)
L_{error}	error in wave length (for iteration)
k	wave number
n	ratio of wave group to wave phase celerity
c	wave phase celerity
c_g	wave group celerity
θ	wave direction relative to shore normal
u_{linear}	peak near bed orbital velocity
A_{linear}	peak near bed orbital excursion
f_w	wave-related friction coefficient
D_{bf}	dissipation by bed friction
γ	breaker criterion
H_m	maximum wave height
H/H_m	wave height to maximum wave height ratio
Q_b	fraction of breaking waves
D_{br}	dissipation by wave breaking
E	wave energy
E_r	roller energy
D_r	roller dissipation
dE_r	change in roller energy
h_{trough}	water depth below wave trough
Q_w	mass flux due to wave motion
Q_r	mass flux due to surface roller
\bar{u}	mean cross-shore flow velocity

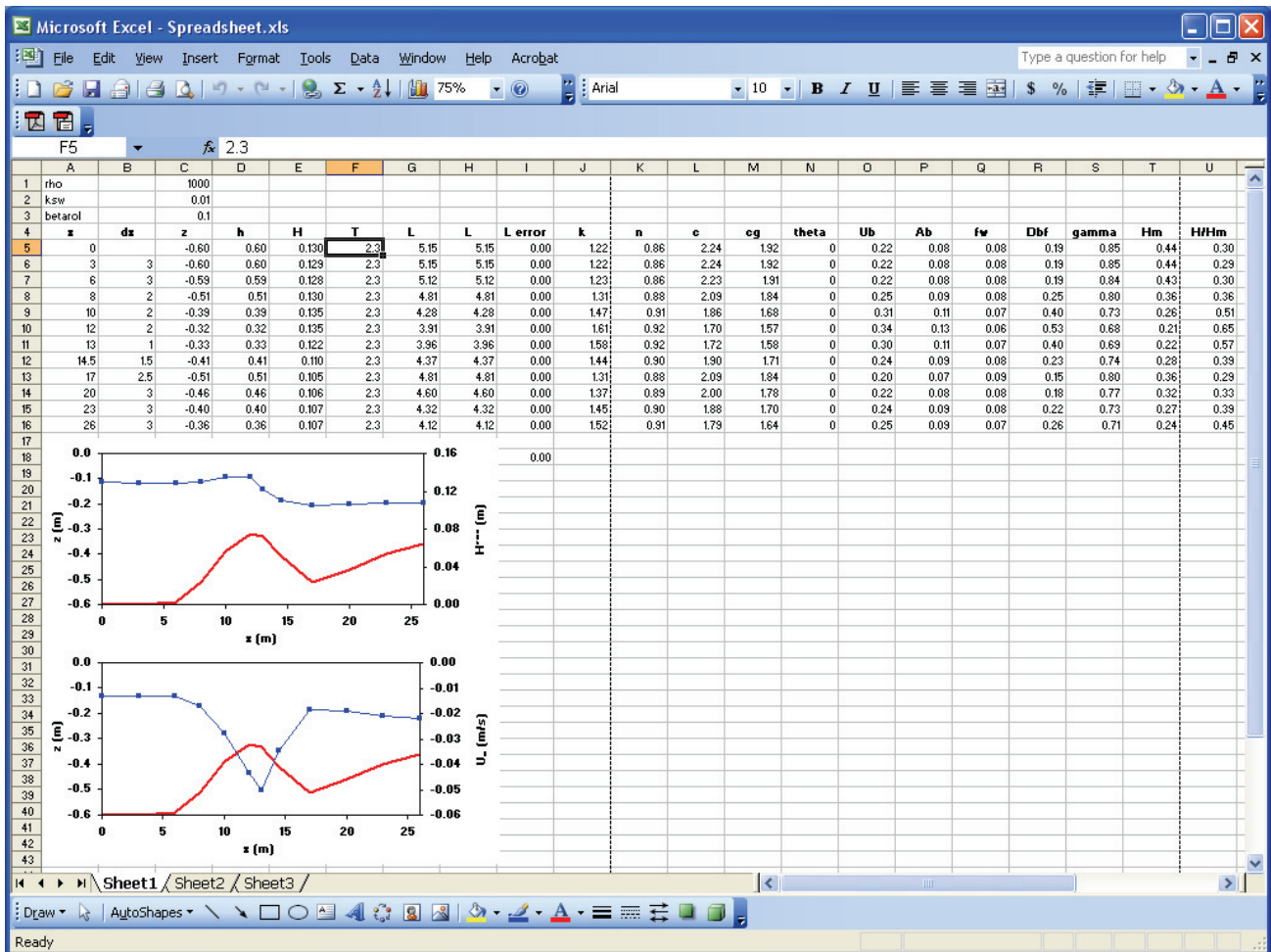


Figure 1. Hydrodynamic model built in an Excel spreadsheet

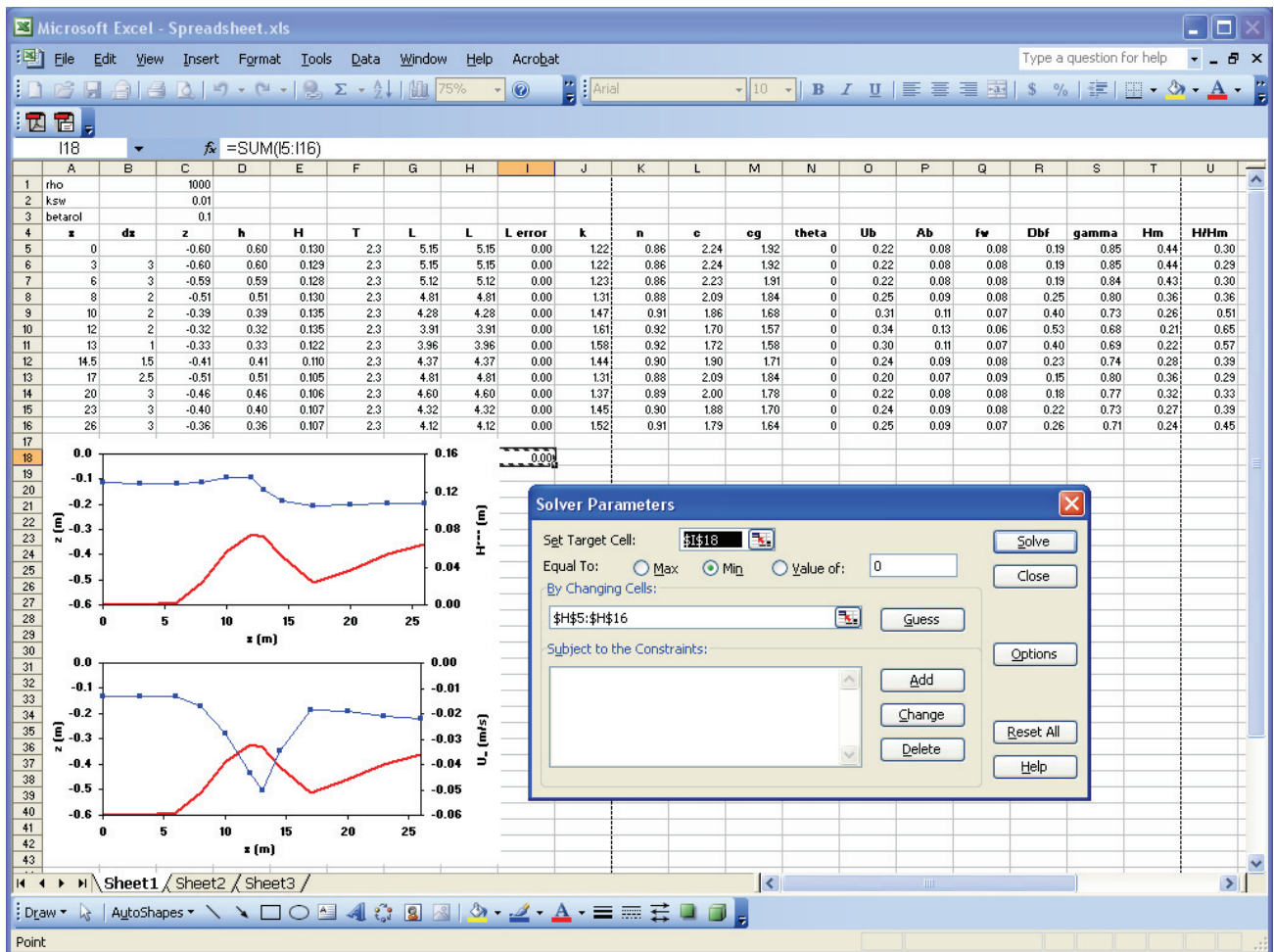


Figure 2. Iteration of wavelengths by minimizing the sum of squared differences.

REFERENCES

- Battjes, J.A., 1975. Modelling of turbulence in the surfzone. ASCE, New York, USA, pp. 1050-1061.
- Battjes, J.A. and Janssen, J.P.F.M., 1978. Energy loss and set-up due to breaking of random waves, Proceedings Coastal Engineering. ASCE, pp. 569-587.
- Deigaard, R., 1993. A note on the three-dimensional shear stress distribution in a surf zone. Coastal Engineering, 20: 157-171.
- Duncan, J.H., 1981. An empirical investigation of breaking waves produced by a towed hydrofoil, pp. 331-348.
- Grasmeijer, B.T. and Ruessink, B.G., 2003. Modeling of waves and currents in the nearshore: parametric vs. probabilistic approach. Coastal Engineering, 49: 185 - 207.
- Isobe, M. and Horikawa, K., 1982. Study on water particle velocities of shoaling and breaking waves. Coastal Engineering in Japan, 25: 109-123.
- Longuet-Higgins, M.S., 1970. Longshore currents generated by obliquely incident sea waves. Journal of Geophysical Research, 75(33): 1-35.
- Longuet-Higgins, M.S. and Stewart, R.W., 1964. Radiation stresses in water waves; a physical discussion, with applications. Deep Sea Research, 11: 529-562.
- Özkan-Haller, H.T. and Kirby, J.T., 1999. Nonlinear evolution of shear instabilities of the longshore current. Journal of Geophysical Research, 104: 25953-25984.
- Putrevu, U. and Svendsen, I.A., 1992. A mixing mechanism in the nearshore region. ASCE, New York, USA, pp. 2758-2771.
- Reniers, A.J.H.M. and Battjes, J.A., 1997. A laboratory study of longshore currents over barred and non-barred beaches. Coastal Engineering, 30: 1-22.
- Roelvink, J.A. and Brøker, I., 1993. Cross-shore profile models. Coastal Engineering, 21: 163-191.
- Ruessink, B.G., Miles, J.R., Feddersen, F., Guza, R.T. and Elgar, S., 2001. Modeling the alongshore current on barred beaches. Journal of Geophysical Research, 106(C10): 22451-22464.
- Stive, M.J.F. and De Vriend, H.J., 1994. Shear stresses and mean flow in shoaling and breaking waves. ASCE, New York, pp. 594-608.
- Svendsen, I.A., 1984. Mass flux and undertow in a surf zone. Coastal Engineering, 8: 347-365.
- Van Rijn, L.C., 1993. Principles of sediment transport in rivers, estuaries and coastal seas. Aqua Publications, Amsterdam.